AFRL-OSR-VA-TR-2014-0057

MULTI BANDGAP PHOTODETECTORS WITH BURIED EPITAXIAL METALLIC CONTACTS

CHRISTOPHER PALMSTROM

THE REGENTS OF THE UNIVERSITY OF CALIFORNIA

01/09/2014
Final Report

AIR FORCE RESEARCH LABORATORY
AF OFFICE OF SCIENTIFIC RESEARCH (AFOSR)/RSE
ARLINGTON, VIRGINIA 22203
AIR FORCE MATERIEL COMMAND

REPORT DOCUMENTATION PAGE

Form Approved
OMB No. 0704-0188

1. REPORT DATE *(DD-MM-YYYY)*	**2. REPORT TYPE**	**3. DATES COVERED** *(From - To)*
30-12-2013	Final Report	04/1/10-09/30/13

4. TITLE AND SUBTITLE

Multi Bandgap Photodetectors with Buried Epitaxial Metallic Contacts

5a. CONTRACT NUMBER

5b. GRANT NUMBER
FA09550-10-0119

5c. PROGRAM ELEMENT NUMBER

6. AUTHOR(S)
Chris Palmstrom

5d. PROJECT NUMBER

5e. TASK NUMBER

5f. WORK UNIT NUMBER

7. PERFORMING ORGANIZATION NAME(S) AND ADDRESS(ES)
University of California, Santa Barbara
Santa Barbara, CA 93106

8. PERFORMING ORGANIZATION REPORT NUMBER

9. SPONSORING / MONITORING AGENCY NAME(S) AND ADDRESS(ES)
Air Force Office of Scientific Research
875 N. Randolph St. PKR 4th Fl
Arlington, VA 22203

10. SPONSOR/MONITOR'S ACRONYM(S)
AFOSR

11. SPONSOR/MONITOR'S REPORT NUMBER(S)

12. DISTRIBUTION / AVAILABILITY STATEMENT

13. SUPPLEMENTARY NOTES

14. ABSTRACT

A method for growing growing single crystal arrays of semimetallic vertical and horizontal erbium antimonide nanorods, nanotrees, and nanosheets embedded within a semiconducting gallium antimonide matrix was investigated. The nanostructures form simultaneously with the matrix and have epitaxial, coherent interfaces with no evidence of stacking faults or dislocations as observed by high-resolution transmission electron microscopy. By combining molecular beam epitaxy growth and in-situ scanning tunneling microscopy, images of the growth surface one atomic layer at a time showed that the nanostructured composites form via a surface mediated self-assembly mechanism that is controlled entirely at the growth front and is not a product of bulk diffusion or bulk segregation. These highly tuneable nanocomposites show promise for direct integration into epitaxial semiconductor device structures, and also provide a unique system in which to study the atomic scale mechanisms for nucleation and growth.

15. SUBJECT TERMS

16. SECURITY CLASSIFICATION OF:			**17. LIMITATION OF ABSTRACT**	**18. NUMBER OF PAGES**	**19a. NAME OF RESPONSIBLE PERSON**
a. REPORT	**b. ABSTRACT**	**c. THIS PAGE**			**19b. TELEPHONE NUMBER** *(include area code)*

Report Type: Final Report (04/01/10 to 09/30/13)
Grant/Contract Title: MULTI BANDGAP PHOTODETECTORS WITH BURIED EPITAXIAL METALLIC CONTACTS
Grant/Contract Number: FA9550-10-1-0119

Surface Mediated Tunable Self-Assembly of Single Crystal Semimetallic Rare-earth-group-V/III-V Semiconductor Nanocomposite Structures

C.J. Palmstrøm
Electrical & Computer Engineering
University of California, Santa Barbara
Santa Barbara, CA 93106-9560

Arrays of metallic nanostructures embedded within a semiconducting matrix are of great interest for applications in plasmonics, photonic crystals, and nanoscale ohmic contacts. Emphasis in this project has been to develop embedded metallic contacts within a single crystal semiconductor structure. An unexpected discovery was that epitaxial nanorods of rare-earth-group-V semimetals with coherent interfaces embedded within a III-V semiconductor matrix could be formed by self assembly during molecular beam epitaxial growth. In-situ scanning tunneling microscopy combined with atomic layer by layer growth studies revealed that nanostructured composites formed via a surface mediated self-assembly mechanism that is controlled entirely at the growth front and is not a product of bulk diffusion or bulk segregation. The structures that form depend critically on the surface diffusion and interfacial energetics. These highly tuneable nanocomposites show promise for direct integration into epitaxial semiconductor device structures, and also provide a unique system in which to study the atomic scale mechanisms for nucleation and growth.

Experimental Procedure and Results

In-situ scanning tunneling microscopy (STM) and ex-situ transmission electron microscopy (TEM) and scanning transmission electron microscopy (STEM) were used to study the atomic scale mechanisms for ErAs:GaAs and ErSb:GaSb nanostructure formation during molecular beam epitaxial (MBE) growth. The experimental setup for the MBE growth and in-situ characterization is shown in Fig. 1. The VG V80H MBE system on the left was used to grow the rare-earth-group-V (RE-V):III-V semiconductor structures. Transfer under ultra-high vacuum (UHV) to the Omicron LT-SPM allowed in-situ STM studies of the grown structures. The samples were also transferred back and forth between the MBE system and STM to investigate the growth process. A second MBE system, a VEECO Gen-III system, was used for many of the ErAs:GaAs studies. This system does not have in-situ characterization facilities and these samples were only characterized ex-situ using TEM and STEM.

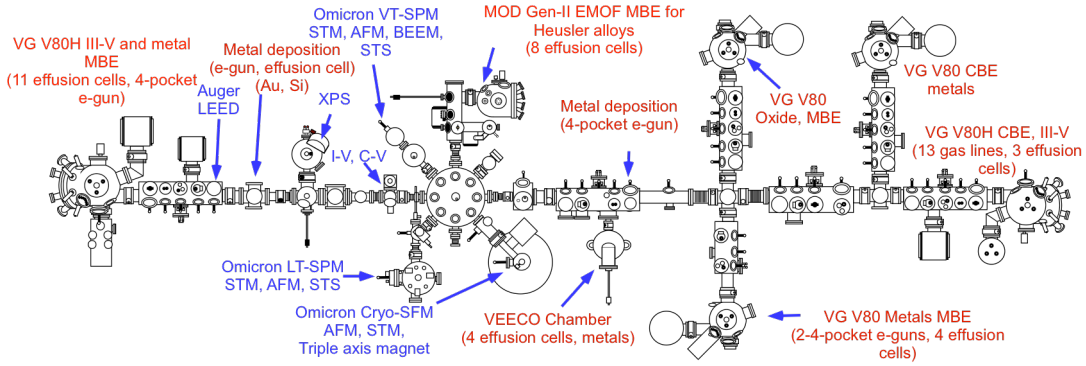

Fig. 1 Schematic of the in-situ growth and characterization system used for these studies. The RE-V/III-V semiconductor composites were grown in the VG v80H MBE system on the left and transferred under UHV to the Omicron VT-SPM for STM measurements.

The driving force for phase separation in the RE-V:III-V systems is analogous to that observed for eutectic (eutectoid) solidification, but instead of occurring at a liquid-solid (solid-solid) interface, here the growth occurs from the vapor at a solid surface. Additionally the mechanism is constrained by the growth surface, with a defined crystal orientation and epitaxial strain, and the resulting nanocomposite is single crystalline with coherent RE-V/III-V interfaces. In making detailed comparisons between the two materials systems, the ErAs:GaAs system is found to be very different from the ErSb:GaSb. The surface diffusion is much faster in the ErSb:GaSb(001) system and the growth surface remains smooth on the atomic scale. Changes in growth conditions can lead to branched nanotrees and

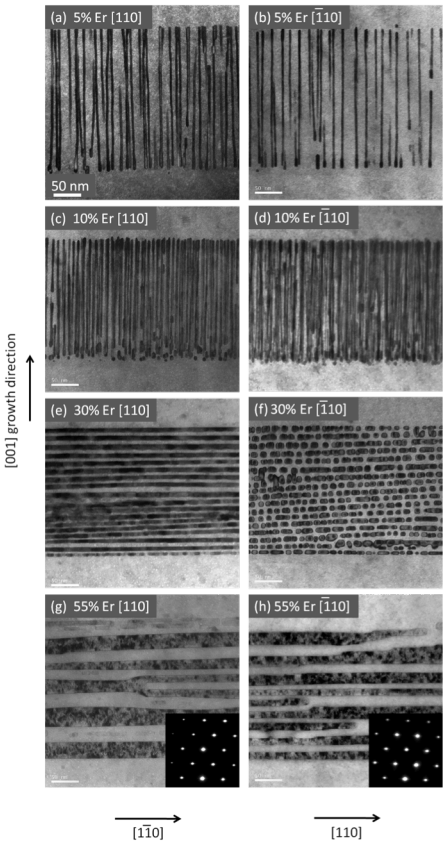

Fig. 2 Bright field TEM images along the [110] and [-110] zone axes of (a,b) a 250 nm $Ga_{0.95}Er_{0.05}Sb$ (001) layer grown at 500 °C. The ErSb phase segregates from the GaSb and forms nanorods aligned along the surface normal. (c,d) TEM images of a $Ga_{0.9}Er_{0.1}Sb$ (001) nanocomposite showing a higher density of vertical nanorods. (e,f) TEM images of a $Ga_{0.7}Er_{0.3}Sb$ (001) nanocomposite. At 30% Er, the ErSb nanorods switch direction and lie in-plane along the [-110] (g,h) TEM images of a $Ga_{0.45}Er_{0.55}Sb$ (001) nanocomposite, forming ErSb nanosheets. (inset) Electron diffraction patterns showing that the nanocomposites are single crystalline.

lamellar nanosheets (Fig. 2)[1]. The driving force for nanorod formation comes from minimizing the total surface energies. The low surface energy surfaces for ErSb are {100} and {110} and {111} for GaSb. Hence the driving forces are for ErSb{100} and GaSb{110} and {111} formation. The total energy minimization depends on the relative surface energy contributions from ErSb and GaSb. For the perpendicular ErSb nanorods growing in GaSb(001) (Er concentrations ~5-15 atomic%), the GaSb surface energetics dominated with the formation of ErSb nanorods with {110} and {100} sides (Fig. 3). For higher Er concentrations, minimization of the ErSb surface energy dominates and horizontal nanorods and nanosheets form [1]. A detailed discussion of the growth mechanism is given in reference [1]. The important results from this study are that the self assembled embedded ErSb nanostructures can be controlled by the growth process and that the overgrown GaSb layers appear free of defects (Fig. 2), opening the possibility for growing stacked $Ga_{1-x-y}Al_xIn_ySb$ semiconductor structures with buried ErSb semi-metallic containing contact layers. By varying x and y, the bandgaps of the semiconducting layers can be controlled allowing for multi bandgap photodetectors to be fabricated.

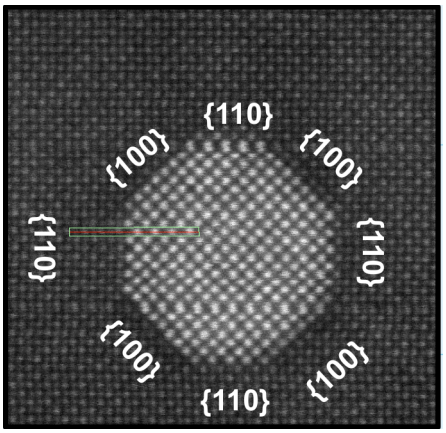

Fig. 3 Plan-view STEM image of an embedded vertical ErSb nanorod in GaSb(001) matrix. Note the octahedral cross-section with {110} and {100} facets.

The current-voltage characteristics of ErSb:GaSb nanocomposites with embedded horizontal ErSb nanowires parallel and perpendicular to the rods are shown in Fig. 4. For reference, measurements of GaSb and ErSb epitaxial layers are also shown.

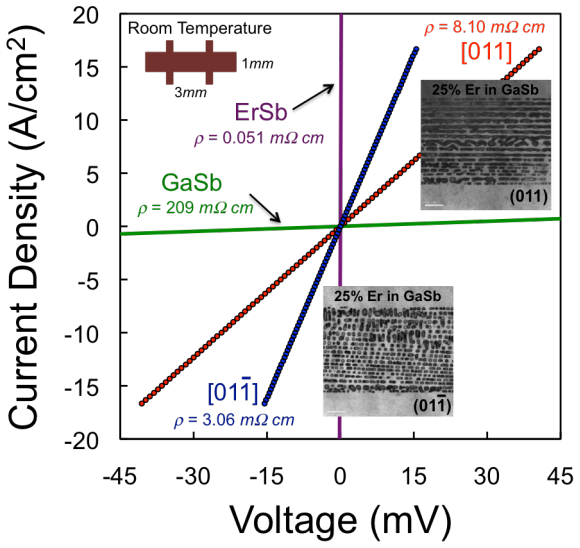

Fig. 4 Current-voltage characteristics parallel and perpendicular to embedded ErSb nanorods in GaSb. For comparison measurements for GaSb and ErSb epitaxial layers are also shown.

The second system studied was the ErAs:GaAs system. The lower atomic surface diffusivity for the ErAs:GaAs(001) system results in significant surface roughening during growth. However, it was found that ErAs nanorods would grow in the [211] direction for growth on GaAs(n11)A (Ga-polar) surfaces, n=2-5{Buehl, 2010 #275;Buehl,

2011 #284}. Hence, by choosing the substrate orientation, the direction of the ErAs nanorods relative to the substrate surface could be controlled. However, nanorods did not form for growth on the GaAs(n11)B(As-polar), n=3=5, surfaces[2,3]. Investigations were made to determine why the ErAs nanorods grew in the [211] direction including in-situ STM and ex-situ TEM studies. Figure 5 shows STM images from the GaAs(311)A and (311)B surfaces. Both the GaAs(311)A and GaAs(311)B surfaces have a (8×1) surface reconstruction. However, the atomic arrangements of the surfaces are very different. Figure 6 shows atomic models for the two surfaces. The one for the GaAs(311)A surface is the one proposed by Wassermeier et al.[4] and the one for the GaAs(311)B surface is one developed from these studies. Both models are consistent with the STM images and electron counting. The smoother and more uniform GaAs(311)A surface is expected to have the higher atomic surface mobility, which is expected to influence MBE growth kinetics.

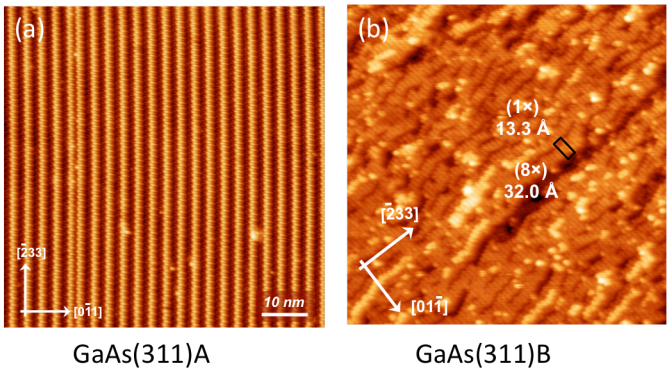

Fig. 5 In-situ STM images of (a) GaAs(311)A and (b) GaAs(311)B surfaces

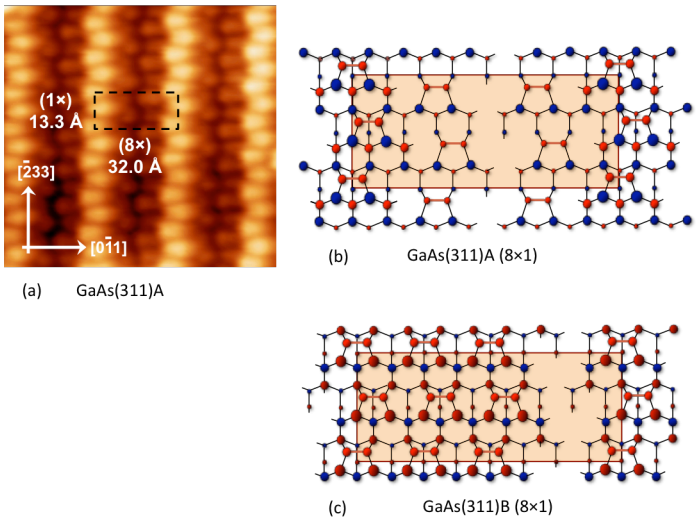

Fig. 6 (a) STM image of GaAs(311)A (8×1) surface reconstruction and predicted atomic models for (b) GaAs(311)A and GaAs(311)B. The red atoms correspond to As and the blue Ga. Both surfaces satisfy electron counting.

The corresponding STM images of the GaAs(311)A and B surfaces after 0.1ML ErAs growth at 580°C are shown in Fig. 7. Both surfaces show the formation of small islands, but in the case of GaAs(311)B deeper pits appear to form on one side of the island. As the initial growth of ErAs involves an Er-Ga exchange reaction[5], the surface clusters are probably GaAs formed from Er-Ga exchange reaction and the pits are likely to be where the ErAs clusters are formed. The formation of these pits and the fact that the nanorods were found to grow in the [211] direction led to the prediction that the ErAs rods are growing on {111} Ga-polar planes. Once an ErAs cluster is formed, further

growth will occur as Er and Ga atoms diffuse towards the cluster. The surface diffusion is expected to be faster along the atomic rows, which run along <-233> direction (Fig. 5). Previous studies have shown that GaAs does not wet the ErAs(100) surface[6] so the GaAs will preferentially grow around the ErAs cluster. The schematic diagrams in Fig. 7 indicate the Ga-polar (111) and (-1-11) planes and how ErAs growth might occur for both GaAs(311)A and GaAs(311)B surfaces. As Er and Ga are supplied and diffuse on the surface, growth of both the ErAs and GaAs occurs. For the GaAs(211)A case, the ErAs nanorod can continually be supplied with Er as the {111} Ga-polar GaAs faceted surfaces around the ErAs nanorod enable fast diffusion of Er even as the GaAs continuously grows (Fig. 7). However, for the GaAs(311)B case, GaAs growth on the {111} Ga-rich facets would result in GaAs overgrowth of the ErAs nanorod (Fig. 7). This is a result of the {111} Ga-polar plane being at an angle >90° to the surface normal. The prediction is therefore that ErAs nanorods can keep growing if the {111} Ga-polar plane normal makes an angle ≤90° to the growth plane normal, but not if the {111} Ga-polar plane normal makes an angle >90° as this would result in GaAs overgrowing the ErAs nanorod. The schematic diagrams in Fig. 7 illustrate this. Figure 8 shows the STM image of the

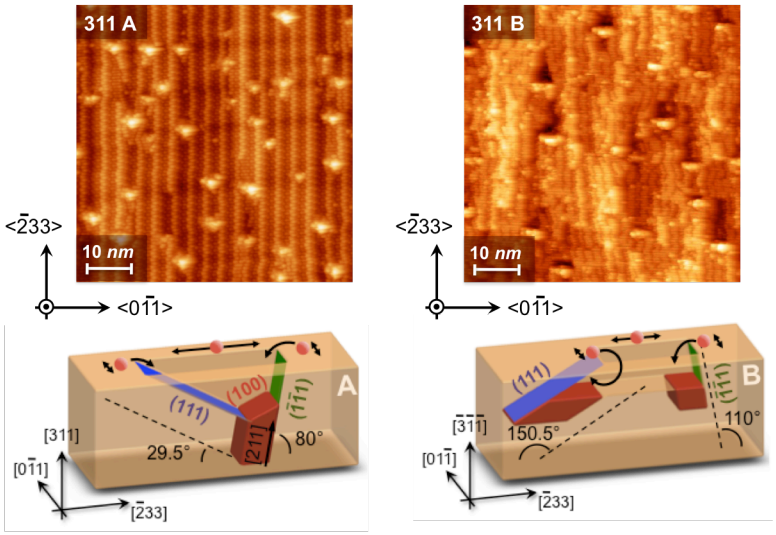

Fig. 7 STM images for 0.1ML ErAs growth on GaAs(311)A and (311)B surfaces. Note the large pits that appear on the surface above the protruding islands for the (311)B surface. The schematics illustrate the position of {111} Ga-rich surfaces and possible surface diffusion of Er atoms for growth of ErAs on the {111} Ga-rich surfaces. Note that in the case of (311)B, an ErAs nanorod could not keep growing as it would be overgrown by GaAs while in the case of the (311)A surface it can continue to grow.

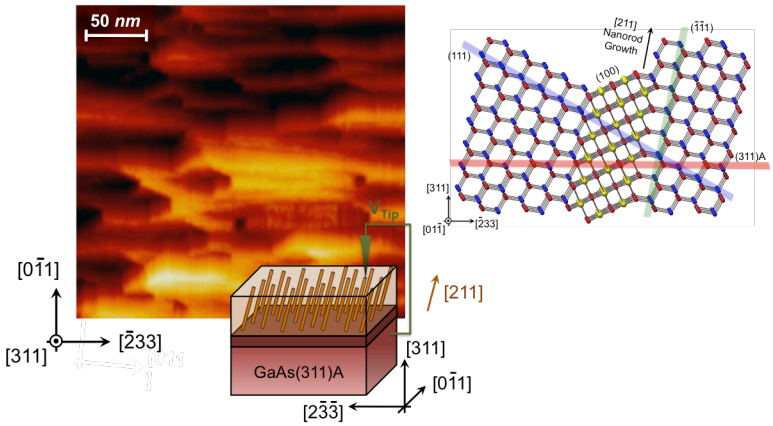

Fig. 8 STM image of a ErAs(6 atomic%):GaAs(311)A surface. The surface is substantially rougher, but ErAs pits are clearly visible on the surface. The ball and stick model on the right shows a potential atomic arrangement for the ErAs nanorod during growth on GaAs(311)A. Note that the low energy ErAs(100) surface is formed on the end of the ErAs nanorod.

surface of a thick ErAs(6 atomic%): GaAs/GaAs(311)A codeposited layer. The pits and surface ridges are clearly visible. The figure also shows a schematic ball and stick model of the ErAs nanorod/GaAs(311)A surface and interface. Note that the nanorod can be terminated with its energetically favorable low energy (100) surface and that the GaAs forms energetically favorable {111} Ga-polar surfaces around the ErAs nanorod. The Ga-rich {111} surface around the ErAs nanorod may also act as a flux mediated epitaxial growth surface for ErAs (analogous to a Vapor-Liquid-Solid type of growth of nanowires).

Further experiments were performed to substantiate the hypothesis that the GaAs {111} Ga-polar surface was critical for the ErAs nanorod formation mechanism. Figure 9 shows how the {111} Ga-polar surfaces are oriented for a number of GaAs surface orientations. For GaAs(n11)B, only the (111)B surface has a {111} Ga-polar plane with a normal <90° to the substrate surface normal. The lack of ErAs nanorod formation for growth on (n11)B, n=3-5, surfaces is consistent with the model prediction. From Fig. 9 one would expect that ErAs nanorod formation should occur for growth on GaAs(211)B, GaAs(111)B and GaAs(100).

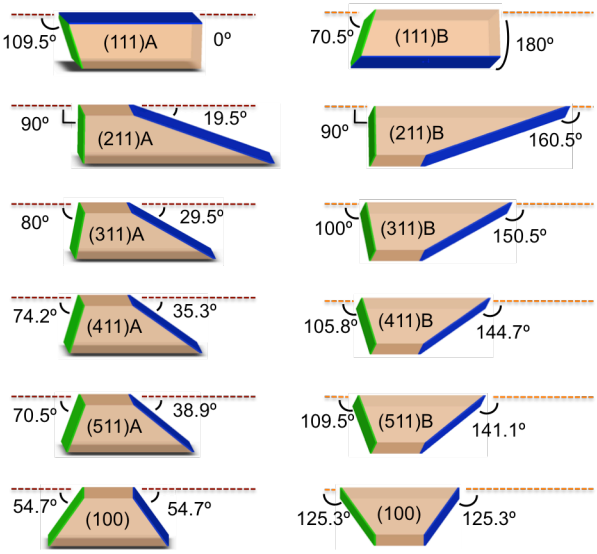

Fig. 9 Schematic of Ga-polar (111) terminated step edges along the [2nn] for a number of GaAs surfaces. Note that for all (n11)B surfaces with n>1, the {111} Ga-polar surfaces make an angle ≥90° with the surface normal.

Figure 10 shows cross-sectional TEM micrographs for growth on GaAs(211)B. The ErAs nanorods may initially start to to grow vertically, but quickly change to grow at a 32° angle to the surface as shown in Fig. 10. This corresponds to growth parallel to the (100) surface rather than the Ga-polar {111}. In-situ reflection high-energy electron diffraction showed that the surface roughened substantially during

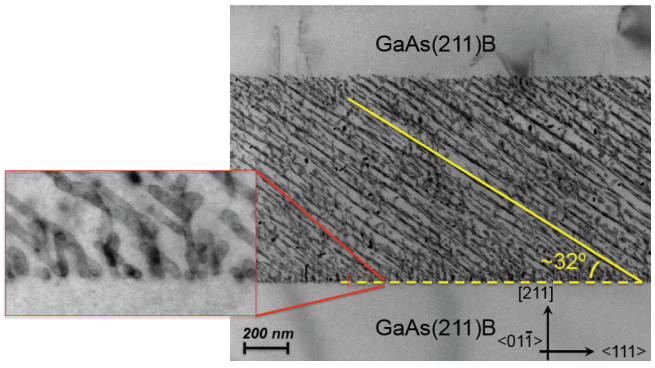

Fig. 10 Cross-sectional TEM micrograph of ErAs(6at%):GaAs /GaAs(211)B heterostructure. Note that some of the ErAs nanorods initiate vertically at the interface and then most are inclined at 32° upon further growth.

growth resulting in (100) facet formation. Fig. 10 also shows that the GaAs overgrowth is of high crystalline quality.

Growth on GaAs(111)B also results in (100) facet formation and ErAs nanorod growth along the (100) surface. Surface roughening is also responsible for the lack of out-of-plane ErAs nanorod growth on the GaAs(100) surface.

Conclusions

A detailed study of ErSb:GaSb and ErAs:GaAs self assembled nanostructure formation has been undertaken. It was demonstrated that through MBE growth control and selection of substrate orientation, semi-metallic nanorods can be controllably grown by self assembly during MBE growth. Although the driving forces for the two systems are similar, the kinetics and relative surface energies are very different. The higher surface diffusivity, better wetting of GaSb on ErSb and smoother growth results in better control of ErSb:GaSb nanostructured material than for ErAs:GaAs.

Buried epitaxial RE-V self assembled nanostructures ranging from perpendicular, angled, branched, and horizontal nanorods as well as nanosheets can be controllably grown using molecular beam epitaxy. High quality III-V semiconductors can be grown on top of the nanocomposites opening up the ability of fabricating buried metallic contact layers for individual contacts for stacked multi bandgap photodetectors.

References

1 J. K. Kawasaki, B. D. Schultz, H. Lu, A. C. Gossard, and C. J. Palmstrøm, *Surface-Mediated Tunable Self-Assembly of Single Crystal Semimetallic ErSb/GaSb Nanocomposite Structures,* Nano Letters **13,** 2895-901 (2013).

2 T. E. Buehl, C. J. Palmstrøm, and A. C. Gossard, *Embedded ErAs Nanorods on GaAs (n11) Substrates by Molecular Beam Epitaxy,* J. Vac. Sci. Technol. B **29,** 03C108/1-4 (2011).

3 T. E. Buehl, J. M. LeBeau, S. Stemmer, M. A. Scarpulla, C. J. Palmstrøm, and A. C. Gossard, *Growth of embedded ErAs nanorods on (411)A and (411)B GaAs by molecular beam epitaxy,* J Cryst Growth **312,** 2089-92 (2010).

4 M. Wassermeier, J. Sudijono, M. D. Johnson, K. T. Leung, B. G. Orr, L. Daweritz, and K. Ploog, *Reconstruction of the GaAs(311) A surface,* Physical Review B **51,** 14721-4 (1995).

5 B. D. Schultz and C. J. Palmstrøm, *Embedded assembly mechanism of stable metal nanocrystals on semiconductor surfaces,* Phys Rev B (Rapid Com) **73,** 241407/1-4 (2006).

6 T. G. Finstad, C. J. Palmstrøm, S. Mounier, V. G. Keramidas, J. G. Zhu, and C. B. Carter, *Initial stages of GaAs growth on $Sc_xEr_{1-x}As$ surfaces,* Mat. Res. Soc. Symp. Proc. **202,** 413-18 (1991).

Publications resulting from this work:

Ph.D. Thesis:

Trevor Buehl Ph.D. Thesis "Semimetallic Nanorods Embedded in High-Index Semiconductors", University of California, Santa Barbara, December 2011
http://search.proquest.com/docview/923627955

Journal Publications:

J. K. Kawasaki, B. D. Schultz, and C. J. Palmstrøm, *Size effects on the electronic structure of ErSb nanoparticles embedded in the GaSb(001) surface,* Phys Rev B **87,** 035419 (2013)

J. K. Kawasaki, B. D. Schultz, H. Lu, A. C. Gossard, and C. J. Palmstrøm, *Surface-Mediated Tunable Self-Assembly of Single Crystal Semimetallic ErSb/GaSb Nanocomposite Structures,* Nano Letters **13,** 2895-901 (2013)

J. K. Kawasaki, R. Timm, K. T. Delaney, E. Lundgren, A. Mikkelsen, and C. J. Palmstrom, *Local Density of States and Interface Effects in Semimetallic ErAs Nanoparticles Embedded in GaAs,* Physical Review Letters **107,** 036806 (2011)

J. K. Kawasaki, R. Timm, T. E. Buehl, E. Lundgren, A. Mikkelsen, A. C. Gossard, and C. J. Palmstrøm, *Cross-sectional Scanning Tunneling Microscopy and Spectroscopy of Semimetallic ErAs Nanostructures Embedded in GaAs,* J. Vac. Sci. Technol. B **29,** 03C104 (2011)

T. E. Buehl, C. J. Palmstrøm, and A. C. Gossard, *Embedded ErAs Nanorods on GaAs (n11) Substrates by Molecular Beam Epitaxy,* J. Vac. Sci. Technol. B **29,** 03C108/1-4 (2011)